

# Reactive neural control for autonomous robots: From simple wheeled robots to complex walking machines

Poramate Manoonpong<sup>1</sup>, Hubert Roth<sup>2</sup>

1) Bernstein Center for Computational Neuroscience, University of Göttingen, Göttingen, Germany,  
poramate@nld.ds.mpg.de, www.bccn-goettingen.de

2) Institut für Regelung und Steuerungstechnik (RST), Elektrotechnik und Informatik, Siegen, Germany,  
roth@rst.e-technik.uni-siegen.de, www.uni-siegen.de/rst

**Abstract** – In this paper, structure and function of reactive neural control for autonomous robots are discussed. The controller utilizing discrete-time neurodynamics is applied to generate various reactive behaviors, like obstacle avoidance (negative tropism) and phototaxis (positive tropism), of two-wheeled robots. Adding additional neural networks leads to an effective modular reactive neural controller, which is then employed to reproduce these reactive behaviors, generally achieved for wheeled robots, also for walking machines with many degrees of freedom.

**Keywords** – Recurrent neural networks, Obstacle avoidance, Phototaxis, Reactive behaviors

## I. INTRODUCTION

Developments of embodied control techniques for autonomous robots, enabling them to interact with their environments or even to adapt themselves into specific survival conditions, have been in progress since 1953 [1], [2], [3], [4], [5], [6]. This robotic domain is attractive because: first, such robotic systems can be used as models to test hypotheses regarding the information processing and control of the systems [7], [8], [9]; second, they can serve as a methodology for the study of sensory-motor coordination [10], [11], [12]; third, they can form the interconnection between biology and robotics through the fact that biologists can use robots as physical models of animals to address specific biological questions while roboticists can formulate intelligent behavior in robots by utilizing biological studies [13], [14], [15], [16]; last but not least, the principle of creating such systems combines various fields of study in order to achieve “autonomous intelligent systems”, which is an active area of research and a highly challenging field.

From this point of view, the work described here continues in this tradition. Thus, in this article, we present small reactive neural control which is firstly developed for two-wheeled robots. The controller allows the robots interact with their environment. That is they can explore their environment by avoiding obstacles (negative tropism), turn toward a light source (positive tropism), and then stop near to it.

Furthermore, this neural controller is integrated with additional neural control modules. This combination leads to a so-called modular reactive neural controller which is then applied to reproduce such reactive behaviors for walking machines with many degrees of freedom. However, the main purpose of this article is not only to demonstrate the autonomous robots performing different types of tropism but also to investigate the analyzable neural mechanisms underlying this approach in order to understand their inherent dynamical properties. Moreover, in this study, we will try to show that reactive neural control can be a powerful technique to better understand and solve sensory-motor coordination problems of systems deriving from simple wheeled robots to complex walking machines.

The next section describes neural modeling employed throughout this work. Section III shows the reactive neural control for two-wheeled robots. Section IV presents the modular reactive neural control for walking machines. Conclusions are given in the last section. Note that in the following description, results and discussions are often being described alongside the structural elements from which they mainly derive, because this better reflects the tight intertwining of structure and function in this approach.

## II. NEURAL MODELING

A biological neuron has a high complexity in its structure and function; thus, it can be modeled at various levels of detail. If one tried to simulate an artificial neuron model similar to the biological one, it would be impossible to work with. Hence an artificial neuron has to be created in an abstract form which still provides the main features of the biological neuron. In the abstract form for this approach, it is simulated in discrete time steps and a neural spiking frequency (or called a firing rate) is reduced to only the average firing rate. Moreover, the amount of time that a signal travels along the axon is neglected. The structure of a standard additive neuron model is shown in Fig. 1.

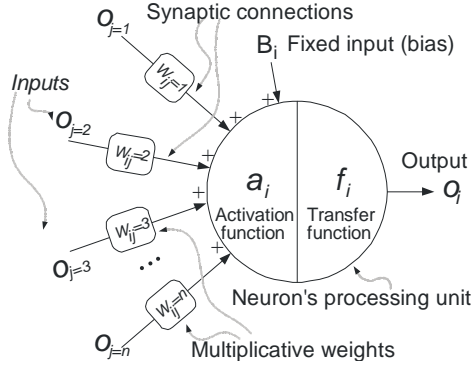


Fig. 1 The structure of an artificial neuron. Each neuron can have multiple input connections, which can originate from other neurons or from a sensor, but there is only one output signal. Then the single output signal can be distributed in parallel (in other words, multiple connections carrying the same signal) to other neurons or to an external system, e.g., a motor system.

The activation and output of the neuron used throughout this work are governed by (1), (2), respectively:

$$a_i(t+1) = \sum_{j=1}^n W_{ij} o_j(t) + B_i \quad i=1, \dots, n, \quad (1)$$

$$o_i = f(a_i) = \tanh(a_i) = \frac{2}{1 + e^{-2a_i}} - 1, \quad (2)$$

where  $n$  denotes the number of units,  $a_i$  their activity,  $B_i$  represents a fixed internal bias term together with a stationary input of neuron  $i$ ,  $W_{ij}$  the synaptic strength of the connection from neuron  $j$  to neuron  $i$ , and  $o_i$  the output of neuron  $i$ . Input units, e.g., sensory neurons, are configured as linear buffers.

### III. REACTIVE NEURAL CONTROL FOR TWO-WHEELED ROBOTS

In this section, we present reactive neural control for two-wheeled robots (see Figs. 2 and 3). The controller serves to eliminate the sensory noise and shape all sensory data for generating phototaxis (positive tropism) and obstacle avoidance (negative tropism) behavior. It is constructed based on the minimal recurrent controller (MRC) structure [17]. The MRC has been developed for controlling only obstacle avoidance behavior of a miniature Khepera robot, which is a two wheeled platform.

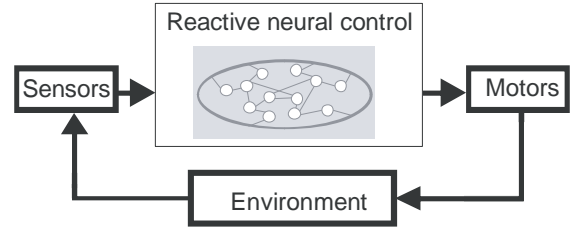


Fig. 2 Diagram of reactive neural control. The controller acts as an artificial perception-action system. That is, it filters and shapes sensory signals. Afterwards it provides outputs directly commanding actuators. As a result, the robot's behavior is produced by interacting with its environment in a sensory-motor loop.

Here, it is adjusted and expanded in the way that it enables a sensor-driven wheeled robot (Fig. 3B) to not only avoid obstacles or escape from a deadlock situation (negative tropism) but also effectively turn toward and approach a light source (positive tropism). By doing so, the reactive neural controller is developed as follows. The principle connection weights  $W_{1, \dots, 4}$  of the network (see Fig. 3A) were manually adjusted with respect to dynamical properties of recurrent neural networks. First, the self-connection weights  $W_{1,2}$  of the output neurons  $O_{1,2}$  were manually tuned to derive a reasonable hysteresis interval on the input space. That is the width of the hysteresis is proportional to the strength of the self-connections (see [18], [19] for details). In this case, the hysteresis effect determines the turning angle for avoiding obstacles and approaching a light source, i.e., the wider the hysteresis, the larger the turning angle. Both self-connections are set to 2.0 to obtain a suitable turning angle (see Figs. 4A and C). Then, the recurrent connections  $W_{3,4}$  between output neurons were symmetrized and manually adjusted to  $-3.5$ . Such inhibitory recurrent connections are formed as a so-called even loop [20], which also shows hysteresis phenomenon (see Fig. 4B). In general conditions, only one neuron at a time is able to produce a positive output, while the other one has a negative output, and vice versa. However, both neurons can show high activation only if their inputs are very high, e.g.,  $> 0.64$  (see Fig. 4B). This guarantees the optimal functionality for avoiding obstacles or escaping from corner and deadlock situations. The sensor values (LDR and IR) are linearly mapped into the closed interval  $[-1, +1]$ . For the LDR sensors, values  $LDR = -1.0$  refers to darkness and  $LDR = +1.0$  to the maximal measurable light intensity. The IR values are  $-1.0$  if no obstacle is detected and value  $+1.0$  represents that an obstacle is near. The left IR sensor signal is used as the first input (*Input1*) to the network while the second input (*Input2*)

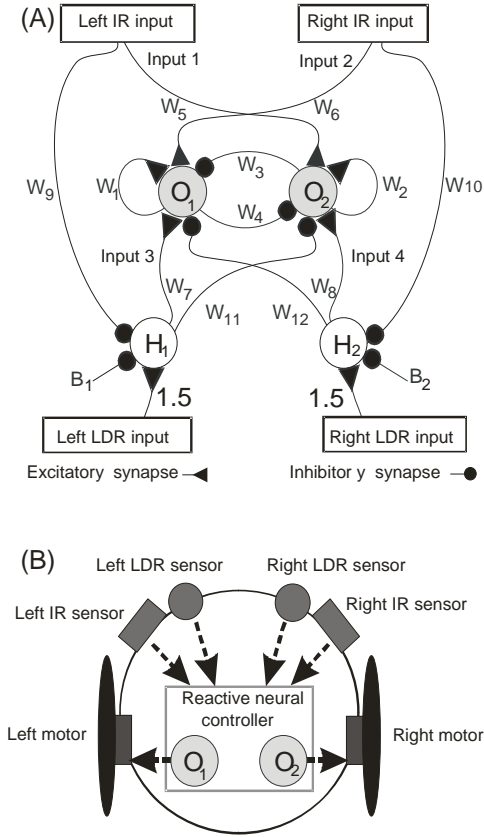


Fig. 3 (A) The reactive neural control for the coordination of positive (LDR sensor signals) and negative (IR sensor signals) stimuli. Its outputs  $O_{1,2}$  are directly used to control left and right motors of the robot, respectively. Note that  $H_{1,2}$  are the hidden neurons of the network. (B) A sensor-driven wheeled robot for experiment with this reactive controller. It consists of two wheels, two infra-red (IR) and two light dependent resistor (LDR) sensors.

corresponds to the right one. Parallely, the left and right LDR sensor signals are provided as the third (*Input3*) and fourth (*Input4*) inputs indirectly passing through hidden neurons  $H_{1,2}$ . Concerning the priority of the sensory signals, here the IR sensor signals are desired to have higher priority than the LDR sensor signals. That is if obstacles and light are detected at the same time, the neural controller has to elicit IR sensor signals and inhibit LDR sensor signals. As a consequence, the obstacle avoidance behavior will be executed instead of the phototaxis. The phototaxis is performed if and only if the obstacles are not detected.

To do so, we set the connection weights  $W_{5,6}$  from *Input1* and *Input2* to the output units to higher values

than the ones  $W_{7,8}$  connecting between the hidden and output neurons. Thus, they were set to  $W_{5,6} = 7.0$  and  $W_{7,8} = 4.5$ . To ensure the optimal functionality for priority setting of the sensory signals, we additionally project two inhibitory connections  $W_{9,10}$  from *Input1* and *Input2* to  $H_1$  and  $H_2$ , respectively, together with a bias term  $B$  at each hidden neuron. These parameters were again manually tuned and were, as a result, set to  $W_{9,10} = -2.0$  and  $B_{1,2} = -1.5$ . Furthermore, two inhibitory synapses  $W_{11,12}$  were extra integrated and set with the same strength of  $W_{7,8}$ , i.e.,  $-4.5$ . These inhibitory cross connections cause that an activated output neuron (showing high activation  $\approx +1$ ) driven by its ipsilateral LDR signal can become deactivated (showing low activation  $\approx -1$ ) if the contralateral LDR signal becomes activated (see Fig. 4D). An important effect of this cross inhibition is to obtain effective phototaxis; i.e., the robot is able to drive forward during performing phototaxis and finally can approach to the source. On the other hand, without these cross inhibition the robot will only try to turn toward the source without performing forwards motion. As a consequence, such a behavior might have difficulties to approach the source. Note that one can optimize the network parameters, for instance by using an evolutionary algorithm [17] but for our purposes here, it is good enough. The complete neural network and its inherent dynamical properties are shown in Figs. 3 and 4, respectively.

This structure and its parameters cause the network to filter, prioritize, and coordinate the different sensory inputs. It can even determine the turning angle as well as the turning direction of the robot by utilizing the hysteresis effect. As a result, the robot can autonomously perform phototaxis and obstacle avoidance behavior through a sensory-motor loop with respect to environmental stimuli. In other words, it will turn toward, approach, and eventually stop near a light source by determining a threshold of the mean value of the left and right LDR sensor signals. At the same time, it will also avoid obstacles if they are detected.

#### IV. MODULAR REACTIVE NEURAL CONTROL FOR WALKING MACHINES

In order to reproduce the desired reactive behaviors presented in the previous section also for a walking machine<sup>1</sup>, additional neural control called *modular neural locomotion control* is required while the reactive

<sup>1</sup> In this article, the six-legged walking machine AMOS-WD06 is used to test the capability of the controller. The description of the walking machine is presented in [18], [19].

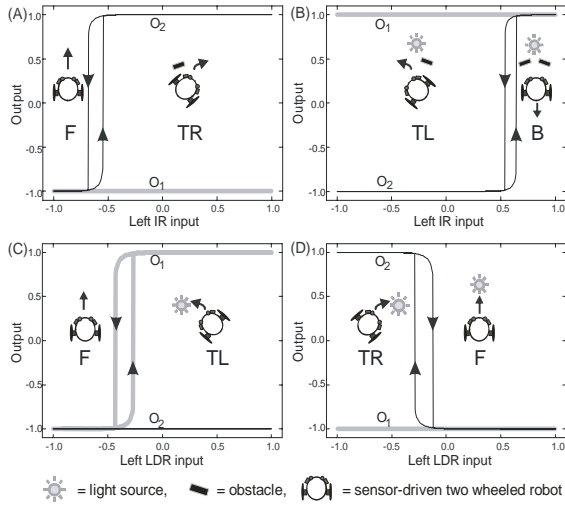


Fig. 4 (A), (B) Hysteresis domain of *Input1* (left IR) for the output neuron  $O_2$  of the network while the other output neuron  $O_1$  shows low  $\approx -1$  and high  $\approx +1$  activation, respectively. All other sensory inputs (right IR, left and right LDRs) are fixed to  $\approx -1$  for case (A) but  $\approx +1$  for case (B). In case (A), the robot drives forward **F** (drawing on the left) as long as  $O_1$  and  $O_2$  give low activation but it turns right **TR** as soon as the left IR input increases to values above  $-0.55$  where only  $O_2$  shows high activation meaning that there is an obstacle on its left (drawing on the right). However, it returns to move forward **F** when the left IR input decreases to values below  $-0.68$  meaning that no obstacle is detected. In case (B), the robot turns left **TL** (i.e., it avoids an obstacle on its right despite it detects a light source in front of it, compare drawing on the left) as long as the value of the left IR input is below  $0.64$  where  $O_1$  has high activation while  $O_2$  shows low activation. Increasing the value of the left IR input above  $0.64$  causes  $O_2$  to become active. The robot then drives backward **B**, i.e., it detects obstacles on both sides (drawing on the right). It will return to turn left **TL** again if the value of the left IR input is below  $0.54$ . (C) Hysteresis domain of *Input3* (left LDR) for  $O_1$  with the other inputs fixed to  $\approx -1$ .  $O_1$  shows high activation if the left LDR input increases to values above  $-0.25$  and returns to low activation if the left LDR input decreases to values below  $-0.4$  while  $O_2$  shows low activation in all cases. As a result, the robot turns left **TL** (drawing on the right) when  $O_1$  shows high activation meaning that it turns toward a light source otherwise it drives forward (drawing on the left). (D) Hysteresis domain of *Input3* (left LDR) for  $O_2$  with the other inputs fixed as all IR inputs  $\approx -1$  and the right LDR input  $\approx +1$ . Here,  $O_2$  shows low activation only if the value of the left LDR input is higher than  $-0.13$  while  $O_1$  gives low activation all the time. However,  $O_2$  will provide high activation if the left LDR input decreases to values below  $-0.28$ . As a consequence, the robot turns toward the source (drawing on the left) and then it is able to move forward if the source is almost in front of it (drawing on the right) causing high activation of both LDR signals. Finally, it can approach to the source. In reverse cases, if the right IR and LDR inputs are varied while the other inputs are fixed, they will derive the same hysteresis effect as shown here.

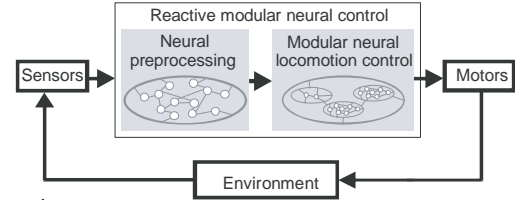


Fig. 5 Diagram of reactive modular neural control. It consists of two main units: neural preprocessing and modular neural locomotion control units. The neural preprocessing unit, obtained from the reactive neural control of the wheeled robot, filters and shapes sensory signals. The preprocessed sensory signals are used to control orienting behavior of a six-legged walking machine through the modular neural locomotion control unit. As a result, the desired phototaxis and obstacle behavior are generated by the interaction between the walking machine and its environment.

neural control described above is used here as a neural preprocessing unit. The entire control structure is shown in Fig. 5. The modular neural locomotion control consists of three subordinate networks<sup>2</sup> or modules (colored boxes in Fig. 6): a neural oscillator network, two velocity regulating networks (VRNs), and a phase switching network (PSN). The neural oscillator network, serving as a central pattern generator (CPG) [18], generates periodic output signals. These signals are provided to all coxa-trochanteral (CTr-) and femur-tibia (FTi-) joints (see Fig. 6) only indirectly passing through all hidden neurons of the PSN. The thoraco-coxal (TC-) joints (see Fig. 6) are regulated via the VRNs. Thus, the basic rhythmic leg movement is generated by the neural oscillator network and the steering capability of the walking machine is realized by the PSN and the VRNs.

Fig. 6 shows the complete network structure together with the synaptic weights of the connections between the controller and the corresponding motor neurons as well as the bias term of each motor neuron. These synaptic weights and all bias terms were manually adjusted to obtain an optimal gait; i.e., a typical tripod gait where the diagonal legs are paired and move synchronously.

This modular neural control can generate different walking patterns which are controlled by the four input neurons ( $I_2, \dots, 5$ ). Furthermore, a self-protective reflex (see [19] for details) can be activated via the input neuron  $I_1$  which will excite  $TR_1$  and  $TL_1$  joints (TC-

<sup>2</sup> A more complete description of each subordinate network is given in [18], [19].

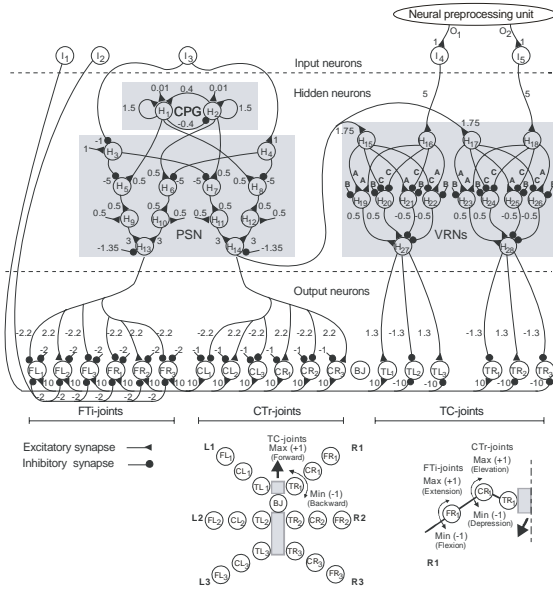


Fig. 6 The modular neural locomotion control of the six-legged walking machine AMOS-WD06 consists of three different neuron groups: input, hidden, and output. Input neurons  $I$  are the neurons used to control walking direction ( $I_{2, \dots, 5}$ ) and to trigger the protection reflex ( $I_1$ ). Hidden neurons  $H$  are divided into three modules (CPG, VRNs, and PSN (see [18], [19] for details)). Output neurons ( $TR$ ,  $TL$ ,  $CR$ ,  $CL$ ,  $FR$ ,  $FL$ ,  $BJ$ ) directly command the position of servo motors. Abbreviations are: BJ = a backbone joint,  $TR(L)$  = TC-joints of right (left) legs,  $CR(L)$  = CTr-joints of right (left) legs,  $FR(L)$  = FTi-joints of right (left) legs. All connection strengths together with bias terms are indicated by the small numbers except some parameters of the VRNs given by  $A = 1.7246$ ,  $B = -2.48285$ ,  $C = -1.7246$ . The location of the motor neurons on the AMOS-WD06 and the movement of its leg joints are shown in the lower picture. Here, the backbone joint functions as a rigid connection. However, it can be modulated by the periodic signal via the PSN or VRNs to perform an appropriate motion, e.g., climbing over obstacles.

joints of the right and left front legs, respectively, see Fig. 6) and all CTr- and FTi- joints and inhibit the remaining TC-joints. Appropriate input parameter sets for the different walking patterns and the reflex behavior are presented in Table I where the first column describes the desired actions in accordance with five input parameters shown in the other columns. Abbreviations are: FDiR and BDiR = forward and backward diagonal motion to the right, FDiL and BDiL = forward and backward diagonal motion to the left, LaR and LaL = lateral motion to the right and the left. Note that marching is an action where all the legs are positioned and held in a vertical position and support is switched between the two tripods.

TABLE I  
INPUT PARAMETERS FOR THE DIFFERENT WALKING PATTERNS AND THE SELF-PROTECTIVE REFLEX BEHAVIOR

Action	$I_1$	$I_2$	$I_3$	$I_4$	$I_5$
Forward	0	1.0	1, 0	-1.0	-1.0
Backward	0	1.0	1, 0	1.0	1.0
Turn right	0	1.0	1, 0	-1.0	1.0
Turn left	0	1.0	1, 0	1.0	-1.0
Marching	0	1.0	1, 0	0.0	0.0
FDiR	0	0.0	0	-1.0	-1.0
BDiR	0	0.0	0	1.0	1.0
LaR	0	0.0	0	0.0	0.0
FDiL	0	0.0	1	-1.0	-1.0
BDiL	0	0.0	1	1.0	1.0
LaL	0	0.0	1	0.0	0.0
Reflex	1	0.0, ..., 1.0	1, 0	-1.0, ..., 1.0	-1.0, ..., 1.0

As shown in Table I, this neural controller can produce at least 12 different actions with respect to the given inputs. Nevertheless, in this article, we simulate the reactive phototaxis and obstacle avoidance behavior representing as orientational responses; i.e., the walking machine will perform orienting walking behavior as soon as it is activated by the positive (light) or negative (obstacles) stimuli. Thus, in the robot walking experiments, the input parameters  $I_{1, \dots, 3}$  are fixed as  $I_1 = 0$ ,  $I_2 = 1.0$ , and  $I_3 = 1$  or  $0$  where the diagonal and lateral motions as well as the reflex action are deactivated. On the other hand,  $I_{4, 5}$  will be stimulated by preprocessed sensory signals  $O_{1, 2}$  coming from the neural preprocessor, respectively (compare Figs. 3A and 6). As a result, the walking machine will behave qualitatively as the wheeled robot does; i.e., it walks forward if no obstacle or light is detected and it will turn right or left with respect to the sensory signals, e.g., turn toward a light source (positive stimuli) but turn away from obstacles (negative stimuli). These reactive behaviors are exemplified in Fig. 7. We encourage readers to see more demonstration at <http://www.nld.ds.mpg.de/~poramate/AMOSWD06.html>.

## V. CONCLUSIONS

This article presents reactive neural network utilizing dynamical properties of recurrent neural networks, e.g., hysteresis phenomena, for behavior control. It is first developed to generate different types of tropism for a two-wheeled robot. Afterwards, the controller is expanded by integrating with other modular neural control in order to also reproduce the desired reactive

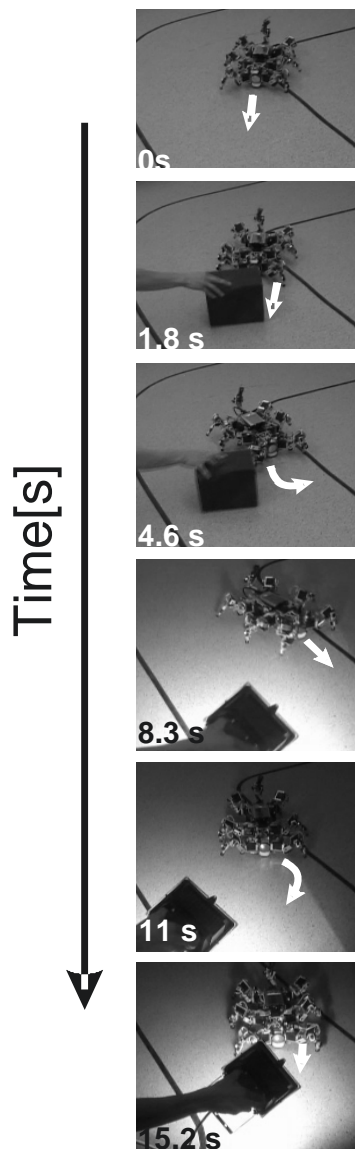


Fig. 7 The phototaxis and obstacle avoidance behavior of the six-legged walking machine AMOS-WD06. The machine walked forwards at the beginning. At around 1.8 s, an obstacle was placed in front of it. The walking machine then turned to the left to avoid it at around 4.6 s (obstacle avoidance behavior). After that, at around 8.3 s, a light source was provided. It turned towards the source at around 11 s. Eventually, it approached and stopped in front of the source (phototaxis).

behaviors for a walking machine. The experimental results show the efficacy of the proposed neural control

approach which can solve sensory-motor coordination problems of the systems deriving from simple to complex ones.

#### REFERENCES

- [1] W.G. Walter, "The Living Brain," New York: Norton, 1953.
- [2] V. Braitenberg, "Vehicles: Experiments in Synthetic Psychology," Cambridge, Massachusetts: MIT Press, 1984.
- [3] R. Pfeifer, M. Lungarella, and F. Iida, "Self-organization, embodiment, and biologically inspired robotics," *Science*, vol. 318, 2007.
- [4] G.A. Bekey, "Autonomous Robots—From Biological Inspiration to Implementation and Control," MIT Press, 2005.
- [5] T.L. Anderson, and M. Donath, "A computational structure for enforcing reactive behavior in a mobile robot," in *Proc. of the SPIE Conference on Mobile Robots III*, vol. 1007, 1988, p. 370.
- [6] R.A. Brooks, and L.A. Stein, "Building brains for bodies," *Autonomous Robots*, vol. 1, no. 1, 1994, pp. 7-25.
- [7] J.L. McKinstry, G.M. Edelman, and J.L. Krichmar, "A cerebellar model for predictive motor control tested in a brain-based device," *Proc. Natl Acad Sci USA (PNAS)*, vol. 103, no. 6, 2006, pp. 3387-3392.
- [8] H. Roth, and K. Schilling, "Hierarchically organised control strategies for mobile robots based on fused sensor data," in *Proc. of Mechatronics*, vol. 1, 1996, pp. 95-100.
- [9] R.I. Damber, and R.L.B. French, "Evolving spiking neuron controllers for phototaxis and phonotaxis," in *Proc. of the EvoWorkshops 2003, LNCS 2611*, 2003, pp. 616-625.
- [10] A. von Twickel, and F. Pasemann, "Evolved neural reflex-oscillators for walking machines," in *Proc. of IWINAC 2005, LNCS 3561*, 2005, pp. 376-385.
- [11] P. Manoonpong, T. Geng, T. Kulvicius, P. Bernd, and F. Wörgötter, "Adaptive, fast walking in a biped robot under neuronal control and learning," *PLoS Computational Biology*, vol. 3, no. 7, 2007, e134.
- [12] F. Iida, and R. Pfeifer, "Sensing through body dynamics," *Robotics and Autonomous Systems*, vol. 54, 2006, pp. 631-640.
- [13] B. Webb, "Can robots make good models of biological behaviour?," *Behavioural and Brain Sciences*, vol. 24, no. 6, 2001, pp. 1033-1050.
- [14] R.E. Ritzmann, R.D. Quinn, and M.S. Fischer, "Convergent evolution and locomotion through complex terrain by insects, vertebrates and robots," *Arthropod structure and development*, vol. 33, no. 3, 2004, pp. 361-379.
- [15] A. Abbott, "Biological robotics: working out the bugs," *Nature*, vol. 445, no. 7125, 2007, pp. 250-253.
- [16] R.D. Beer, R.E. Ritzmann, T. McKenna, (eds.), "Biological Neural Networks in Invertebrate Neuroethology and Robotics (Neural Networks, Foundations to Applications)," Boston, Massachusetts: Academic, 1993.
- [17] F. Pasemann, M. Huelse, and K. Zahedi, "Evolved neurodynamics for robot control," in *Proc. European Symposium on Artificial Neural Networks*, vol. 2, 2003, pp. 439-444.
- [18] P. Manoonpong, "Neural Preprocessing and Control of Reactive Walking Machines: Towards Versatile Artificial Perception-Action Systems," *Cognitive technologies*, 2007.
- [19] P. Manoonpong, F. Pasemann, and F. Woergoetter, "Sensor-driven neural control for omnidirectional locomotion and versatile reactive behaviors of walking machines," *Robotics and Autonomous Systems*, vol. 56, no. 3, 2008, pp. 265-288.
- [20] F. Pasemann, "Discrete dynamics of two neuron networks," *Open Systems and Information Dynamics*, vol. 2, 1993, pp. 49-66.

The Fifth International Conference on Neural Networks and Artificial Intelligence  
May 27-30, 2008, Minsk, Belarus